Intrinsic defects doping in spray deposited $CuInS_2$ thin films

T. SAHRAOUI[a,*], M. ADNANE[a], D. CHAUMONT[b], S. HAMZAOUI[a]
[a] *LMESM-Département de Technologie des Matériaux-Faculté de Physique, Université d'Oran des Sciences et de la Technologie-Mohamed Boudiaf BP 1505 Oran, Algeria*
[b]*Laboratoire ICB, Université de Bourgogne- Dijon, France*

Thin layers of copper indium disulfide $CuInS_2$ were prepared on corning glass substrate at 300°C by the chemical reactive spray process from an aqueous solution containing cuprous and indium chlorides $CuCl_2$, $InCl_3$ and thiourea $SC(NH_2)_2$. The Cu/In molar ratio is varied from 0.5 to 1.5 whereas the Sulfur concentration was maintained constant at 0.04 mol/l in the precursor's solution. Films bulk composition and surface morphology were analyzed by Electron Microprobe Analysis (EMPA) and Scanning Electron Microscopy (SEM).Surface topography of submicron crystallites were observed by Atomic force microscopy. Electrical conductivity was investigated by hot probe and hall-effect methods. It was found that films grown under Cu rich condition have p type conductivity with a hole concentration of order of 10^{20} cm^{-3} in the bulk. The resistivity of the films was found to decrease with the increase of the copper to indium ratio in the precursor solution. Raman spectrum of copper deficient films show A_1 (290 cm^{-1}) and A^*_1 (305 cm^{-1}) vibration modes due to Chalcopyrite (CH) and Copper Gold (Au /Cu) ordering in the films.$CuInS_2$ possesses a number of intrinsic (native) defects which controls the doping of the films. The initial composition of precursors solution is critical to determine the nature of defects (interstitials, vacancy or substitution) and the conductivity type of the deposited films. $CuInS_2$, thin layers deposited from copper–rich solutions resulted in p type CIS films with a high conductivity. The objective of this work is to investigate the role of cations concentration ratio in the sprayed solution on the electrical, optical and structural properties of $CuInS_2$ deposited layers.

(Received November 7, 2017; accepted November 29, 2018)

Keywords: Spray, Thin films, Native defects, SEM, EDX, Electrical properties, Optical properties

1. Introduction

Copper Indium disulfide ($CuInS_2$) is known to be a potential absorber material for thin film solar cells due to its high absorption coefficient ($\approx 10^5 cm^{-1}$) and optical band gap which ranges from 1.3 to 1.5eV for $CuInS_2$ polycrystalline thin films [1]. Theses values are close to the optimal value for the solar cell absorber materials. $CuInS_2$ thin films have been prepared by a variety of techniques like flash evaporation RF sputtering chemical vapour deposition and spray pyrolysis [2-5]. For economic reasons, it should be very interesting to achieve these thin films using a cheap deposition technique. Of these, spray pyrolysis is a simple and inexpensive technique suitable for the production of large area and homogeneous films [6]

2. Experimental

The chemical reactive spray technique was used to make $CuInS_2$ thin films. The gas (Nitrogen) and liquid (Solution) flows were respectively fixed at 5 l/mn and 20 ml/mn. As substrate we used Soda lime glass SiO_x (Corning glass). Aqueous solutions of copper chloride dihydrate ($CuCl_2$, $2H_2O$, 95% Sigma Aldrich) Indium chloride ($InCl_3$, 98% Sigma Aldrich) and thiourea ($SC(NH_2)_2$, 95% Sigma Aldrich) were used as precursors. These solutions were mixed in appropriate portions to reach a copper to indium molar ratio (Cu)/(In) 0,5 to 1,5 and a sulphur to copper molar ratio (S)/(Cu) of 4 in the final solution. To avoid undesirable precipitation, the $CuCl_2$ and $SC(NH_2)_2$ were firstly mixed under magnetic stirrer during 5mn and then the $InCl_3$ solution added. The distance between the spray nozzle and the substrate is 25 cm. Substrate temperature was kept constant at 300°C. Surface topography and cross section of the films were examined by scanning electron microscopy (SEM) using JEOL JSM6610LA (20keV).The average roughness of the surface in the submicron range is measured by AFM (JEOL JSPM 5200).

The composition of all samples were obtained by electron microprobe analysis (EMPA) using Silicon dry detector (SDD) mounted on scanning electron microscope, the accelerating voltage was 20 kV and the beam current 1nA. The electrical properties of the films were investigated by four probe Van der Pauw method and Hall effect measurements on (HMS300, Ecopia). The conductivity type and concentration of majority carriers were estimated by hot probe method using a Weller soldering iron as heater and FLUKE 8854A Digital Multimeter for recording the Thermoelectrical Voltage.

Reflectance and transmittance spectra were obtained using SPECORD 210 PLUS spectro-photometer equipped with 75-mm integrating sphere.

Micro Raman spectroscopy (HORIBA HR 240) was used as non destructive method to analyze the film surface, the crystalline quality and possibly the existence of secondary phases in the deposited films.

3. Results and discussion

3.1. Surface morphology and elemental composition

Fig. 1 shows the SEM micrographs of CIS surface. The films are homogeneous with crystallite of uniform shape. The layers were well adherents to the soda –lime glass substrate.

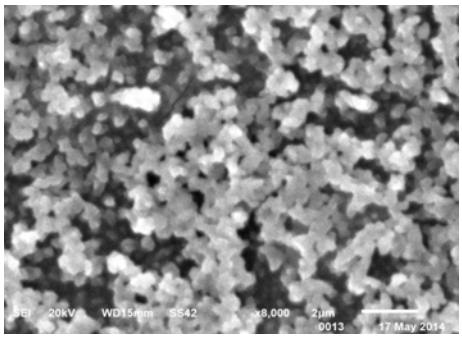

(a)

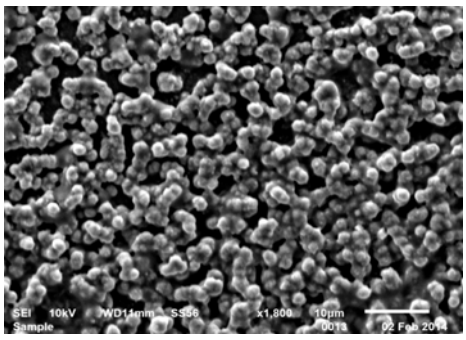

(b)

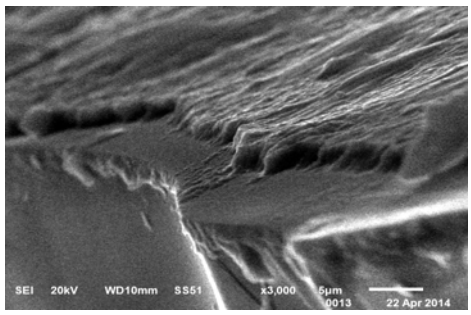

(c)

Fig. 1. Surface (a), (b) and cross –section (c) SEM images of $CuInS_2$ films

The image of In–rich film in Fig. 1 (a) shows a fine-grained surface with agglomerated areas separated by voids. The grains are formed by submicron crystallites.

A better crystallized structure is shown in Fig. 1 (b) for CIS films obtained from Cu-rich sprayed solutions. The crystallites are spherical in shape.

The grain size increases from 2 to 10 μm as the cation molar ratio (Cu)/(In) increase from 0.5 to 1.5 in the initial solution. The cross section of $CuInS_2$ film is presented in Fig. 1 (c). The thickness of deposited films is estimated to vary from 1 to 2 μm. In order to know more about the form of submicron crystallite, we have observed the layers by AFM.

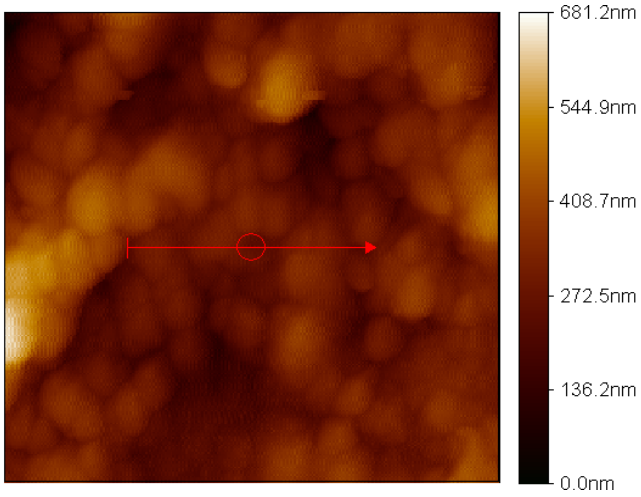

(a)

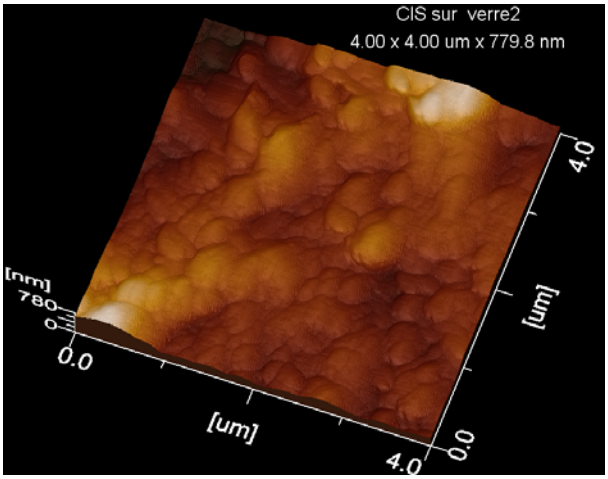

(b)

Fig. 2. AFM images 2D (a) and 3D(b) of CIS films

Fig. 2 (a) shows 2D AFM image of (4×4)μm² area for CIS sample of Fig. 1 (a). The particles have a rounded shape and a distribution size in the range 50–200 nm. The root mean square (RMS) of surface roughness is 30 nm. Fig. 2 (b) shows the topography of the analyzed area. The depth is about 800 nm.

The molar concentration and elemental composition of the films are presented in Table 1, for In rich (CIS (a)) and Cu rich (CIS (b)) precursor solutions.

Table 1. Molar concentration (mol/l)of precursor solutions and the elemental composition (atom%)in the deposited $CuInS_2$ films

	$CuCl_2$	$InCl_3$ (mol/l)	$SC(NH_2)_2$	S	Cu (atom%)	In
CIS(a)	0.01	0.02	0.04	42.19	24.41	27.40
CIS(b)	0.015	0.01	0.04	51.95	30.39	22.61

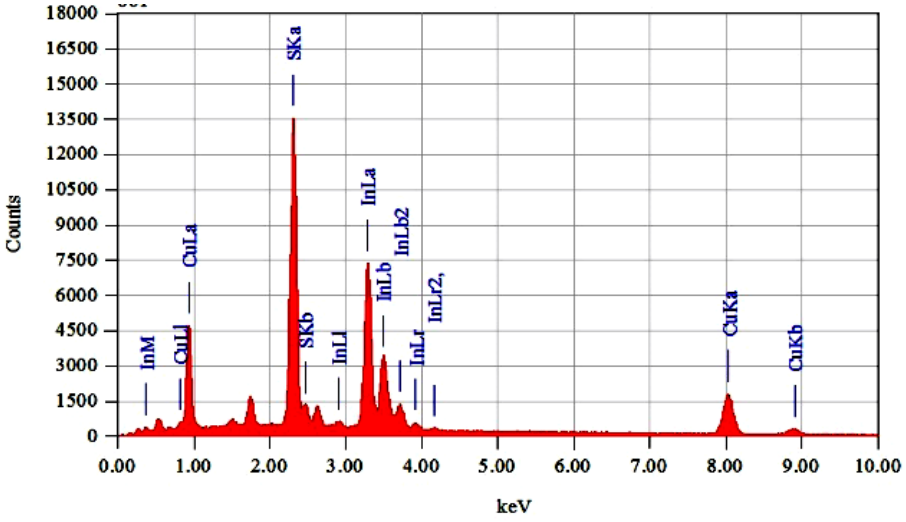

ZAF Method Standardless Quantitative Analysis
Fitting Coefficient : 0.0458

Element	(keV)	Mass%	Sigma	Atom%	Compound	Mass%	Cation
Cu K	8.040	24.84	0.10	24.22			
S K	2.307	25.31	0.04	48.89			
In L	3.285	49.85	0.11	26.89			
Total		100.00		100.00			

(a)

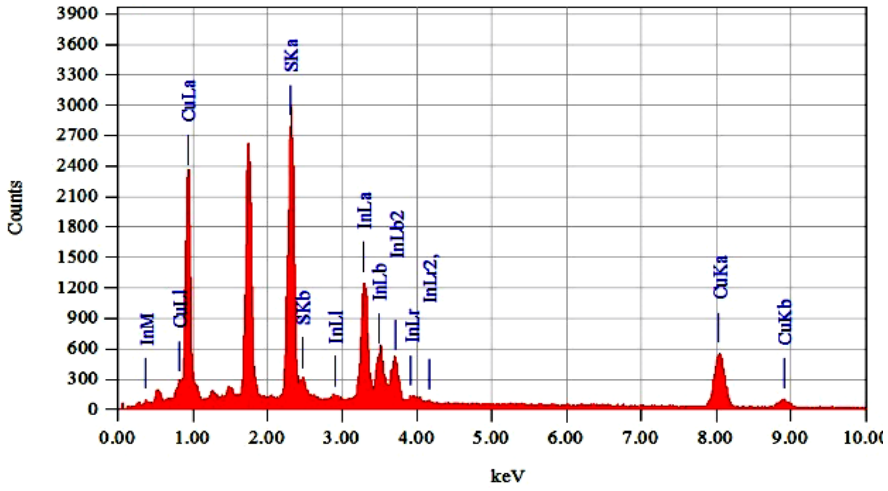

ZAF Method Standardless Quantitative Analysis
Fitting Coefficient : 0.2018

Element	(keV)	Mass%	Sigma	Atom%	Compound	Mass%	Cation
S K	2.307	25.53	0.09	46.89			
Cu K	8.040	36.06	0.24	33.42			
In L	3.285	38.41	0.22	19.70			
Total		100.00		100.00			

(b)

Fig. 3. EDAX analysis spectrum of Cu poor (a) and Cu rich (b) $CuInS_2$ films

Fig. 3 shows the EDAX analysis of two CIS samples. We prepared films by varying the cation molar ratio (Cu)/(In) in the precursor solution. Composition deviations of $CuInS_2$ can be expressed by molecularity ratio x = [Cu]/[In] and the stoichiometry parameter y=2[S]/([Cu]+3[In]). $CuInS_2$ is of p type conductivity in films with an excess S or Cu atoms content (x>1 and y>1). Sulfur deficient or In rich films show n type conductivity (x<1 and y<1).

Table 2. Chemical composition (atom %), molecularity x and stoichiometry y parameters for six CIS samples

Sample	% at. Cu.	% at. S	% at. In		x= [Cu]/[In]	y=2[S]/([Cu] + 3[In])	Conductivity
C1	24.7	47.0	28.3		0.87	0.86	N
C2	26.6	48.4	24.9		1.07	0.95	P
C3	25.5	47.4	27.1		0.94	0.89	N
C4	36.2	46.1	17.7		2.05	1.03	P
C5	24.4	52.9	22.6		1.07	1.14	P
C6	25.9	48.2	25.9		1.00	0.93	P

Table 2 presents the chemical composition, the molecularity and stoichiometry parameters and the related type conductivity for six CIS deposited films. Fig. 4 represents the Gibbs phase triangle for Cu-In-S system at room temperature [7]. The inset in Fig. 4 shows the detail calculated positions for samples C1-C6 (after x and y values given in Table 2). The ternary $CuInS_2$ possesses 12 possible intrinsic point defects which controls the doping of the films. In the Cu-rich region of the phase diagram ([Cu]/[In]>1) p-type conductivity occurs via substitutional Cu_{In} atoms or vacancies V_{In} whereas the In–rich region shows n-type conductivity due to interstitials In_i or place exchange In_{Cu}. The situation is complicated in the phase diagram region where (x<1 and y>1) by the presence of point defects with opposing doping effects. Some point defects tend to form complexes with very low energy formation. Zhang and coworkers [8] predicted for the $CuInSe_2$ system an electrically neutral defect complex ($2V_{Cu}^{-}+ In_{Cu}^{2+}$). The films are intrinsic (high resistivity) or have p or n conductivity. Table 3 resumes the different point defects in sprayed films and their related conduction type [9].

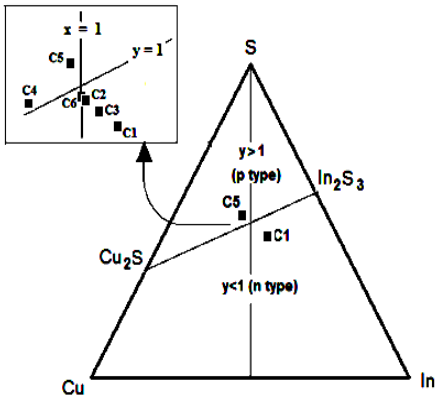

Fig. 4. Ternary phase Diagram of Cu-In- S the inset shows position of samples C1-C6

Table 3. Intrinsic point defects and conductivity in $CuInS_2$ [9]

Point defect		Conduction type
Interstitials	Cu_i	n
	In_i	n
	S_i	p
Place exchange	S_{In}, Cu_{In}, S_{Cu}	p
	Cu_S, In_S, In_{Cu}	n
Vacancies	V_{In}	p
	V_S	n
	V_{Cu}	p

3.2. Electrical measurements

Hot probe measurements confirm the p-type conductivity of samples C2, C4, C5 and C6. The inset of Fig. 3 shows that samples C2 and C6 (y<1) were relatively close to the pseudo binary Cu_2S-In_2S_3 tie line and exhibit p type conduction. We used the conventional hot probe method at 200°C to measure thermo electrical voltage of samples C4, C5 and C6 (Fig. 5).

This thermo EMF is due to the diffusion of thermo excited majority carriers in the semiconductor from the hot to the cold electrode. The thermo EMF varies from -0,5 mV to -2 mV for as deposited samples C6 through C4. This findings may be related to the difference of hole concentration which is of order of 10^{22} cm^{-3}, 10^{20} cm^{-3} and $<10^{20}$ cm^{-3} for C4, C5 and C6 samples respectively (Table 4).

The evolution of measured thermoelectrical voltage for sample C3 (n type) as function of time is illustrated in Fig. 6, for different hot electrode temperature.

The charge density Q of carriers excited by heated electrode is related to the measured thermo electrical voltage V through the formula [10]:

$$Q = -\frac{V.2\pi\varepsilon_0\varepsilon_r\sqrt{4\pi Dt}}{qL^2} \quad (1)$$

Here, D is the diffusion coefficient of the charged carriers; ε_r is the relative permittivity of $CuInS_2$ film and L the spacing between hot and cold electrodes.

The positive thermo-electrical voltage obtained for sample C3, indicates the negative polarity of carriers. On the other hand Q increases with increasing hot electrode temperature [10]. This is indicated by increasing of measured voltage in Fig. 6.

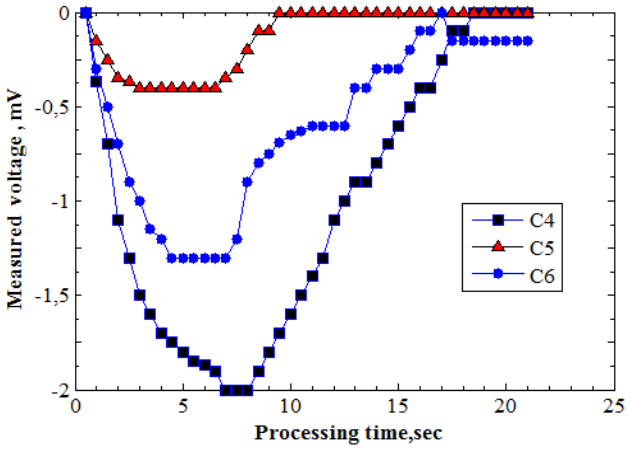

Fig. 5. Measured voltage of thermo excited carriers(holes), Hot electrode temperature (200°C).

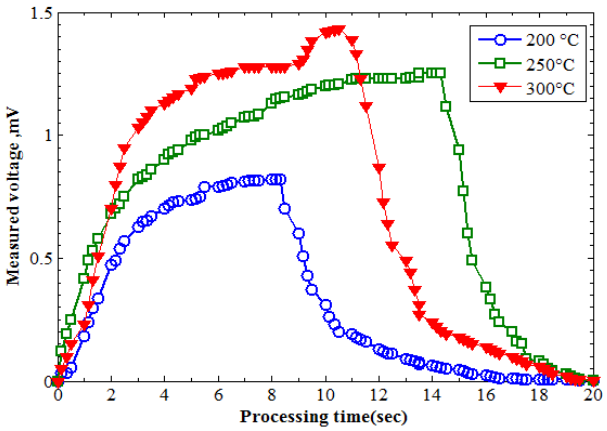

Fig. 6. Measured voltage for n-type CIS (C3) in various hot electrode temperature

The resistivity of $CuInS_2$ films was determined using four probes Van der Pauw configuration. The values ranging 10^{-3} to 10^{-1} Ω.cm. The lowest value ($3{,}5.10^{-3}$ Ω.cm) is obtained for Cu rich films (Cu/In=2.05) as shown in Table 4. The resistivity decreases with the increase of copper content in the films. Several authors have studied $CuInS_2$ and shown that the electrical resistivity can vary by several orders of magnitude according to the deposition technique adopted. For spray deposited p-type $CuInS_2$, annealed in Nitrogen N_2 a value of 3×10^{-2} Ω.cm was reported [11].

High conductivity of Cu rich samples is due to the presence of highly conducting Cu_xS phase at the surface of the films. Hall effect voltage V_H ,using Van der Pauw configuration, is obtained at room temperature (300°K) by forcing a current of 50 µA to flow between two opposite nodes of the sample and then the voltage is measured on the other opposite nodes.

The applied magnetic field was 1 Tesla. The resistivity, carriers concentration and mobility were presented in Table 4. The hole concentration increases with the copper content in the films. The degenerately high hole concentration (of order of 10^{20} cm^{-3}) is attributed by Tiwari and al to the presence of Cu_2S and CuS phases [12].

Table 4. Resistivity, concentration, Hall mobility and type of conduction of $CuInS_2$ thin films

The high concentration of free carriers and low mobility can be attributed to the presence of structure defects which introduce recombination centers in the band gap.CIS Samples	[Cu]/[In]	Electrical resistivity x 10^{-2} (Ωcm)	Bulk concentration N(cm^{-3})	Hall Mobility (cm^2/V.s)	Conduction type
C4	2.05	0.35	2.57×10^{22}	0.07	P
C5	1.07	12.30	1.26×10^{20}	0.40	P
C6	1.0	0.58	9.08×10^{19}	11.8	P

3.3. Optical measurement

Fig. 7 (a) and (b) presents transmittance and reflectance spectrum of $CuInS_2$ samples in the visible and near IR wavelength range [400-1100 nm]. Absorption in $CuInS_2$ takes place by intertitials and substitutional atoms (intrinsic defects) present in the deposited films. The transmittance with absorption but no cos oscillations is given by the relation [13]:

$$T = \frac{(1-R)^2 e^{-\alpha d}}{(1-R^2 e^{-2\alpha d})} \quad (2)$$

From the above equation one can derive the absorption coefficient expression:

$$\alpha = -\frac{1}{d}\ln\left[\frac{\sqrt{(1-R)^4 + 4T^2R^2} - (1-R)^2}{2TR^2}\right] \quad (3)$$

The absorption coefficient α is related to the energy gap according to the equation [14]:

$$\alpha h\nu = A(h\nu - Eg)^n \quad (4)$$

A is a constant, υ the frequency of incident beam, Eg is the optical band gap and n characterizes the nature of band transition. Indeed, n=1/2 and 3/2 corresponds to direct allowed and direct forbidden transitions respectively [15]. $CuInS_2$ is a direct band gap semiconductor and the optical gap can be deduced using the $(\alpha h\nu)^2$ versus photon energy hν plot.

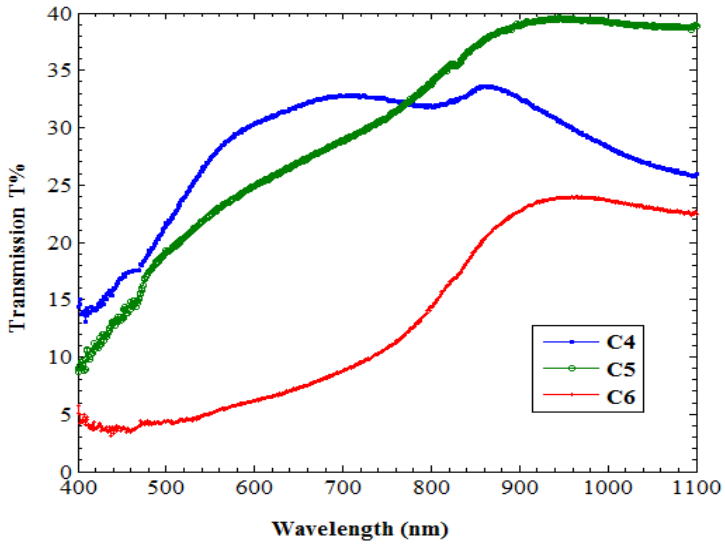

(a)

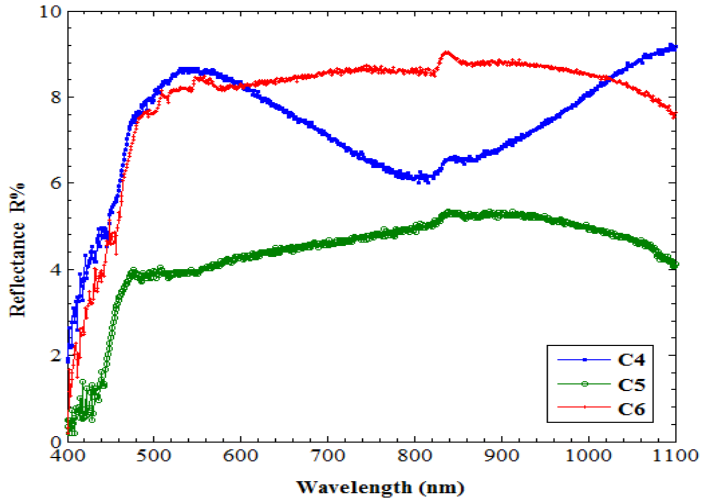

(b)

Fig. 7. (a) Transmission and (b)reflectance spectra of $CuInS_2$ films

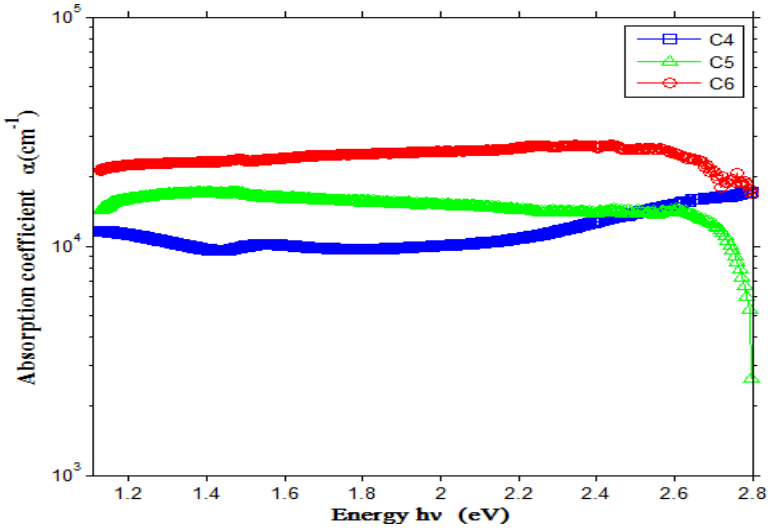

(a)

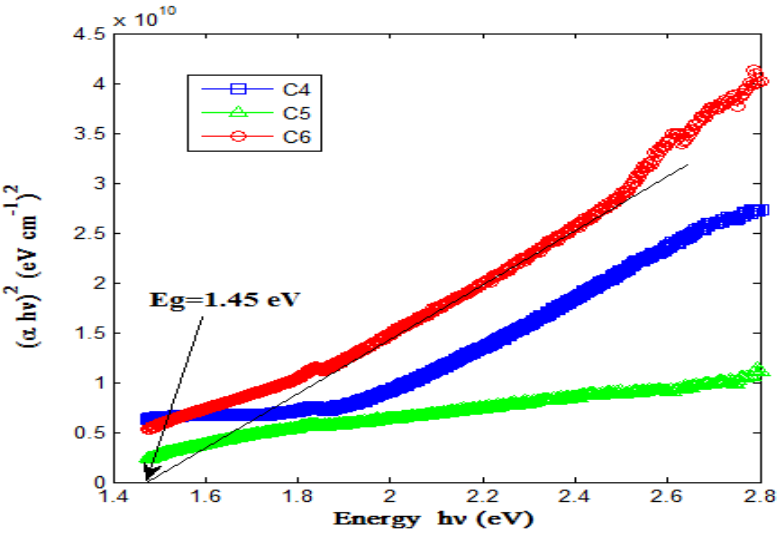

(b)

Fig. 8. Absorption coefficient (a) and $(\alpha h\nu)^2$ versus $h\nu$(b)plots

We noticed in Fig. 6 that the transmission spectra do not exceed 40% for sample C5 and reflection is only 5%. This suggested that a big part (55%) of light is absorbed in the sample. The absorption coefficient presented in figure 8.a for C4, C5 and C6 samples is of the order of 10^4 cm^{-1}. This shows that the deposited CIS films are good light absorbers in the visible range.

The extrapolation of straight line from high absorption region in Fig. 8 (b) indicate a direct band gap of 1,45 eV for films with a stoichiometric composition (CIS–C6), close to the values given in literature [16]. For non stoichiometric C4 and C5 samples, extrapolation leads to E_g =1,9 and 2,1 eV respectively.

3.4. Raman spectroscopy

Micro Raman measurements using the red line 1,916 eV (λ=650 nm) of an Ar^+ ion laser as excitation source were conducted for structural investigations of as deposited $CuInS_2$ thin layer.

The initial molar ratio in precursor solution was (Cu)/(In) = 0.9. Laser power is held below 1 mW to reduce sample heating and to avoid induced crystallization in the films.

High power density can damage the chemical or structural properties of the material .This is especially crucial for $CuInS_2$ as the absorption coefficient of the material is very high [19].

Raman spectrum in Fig. 9 exhibit three intensive bands corresponding to Raman shift 250 cm^{-1}, 305 cm^{-1} and 348 cm^{-1}. The most intensive peak at 305 cm^{-1} is attributed to A^*_1 phonon vibration mode of $CuInS_2$ with CuAu (CA) ordered phase.

Alvarez and coworkers [20] observed a similar behavior from polycrystalline $CuInS_2$ samples prepared by co evaporation and attributed this finding to the Cu poor content of the film. In addition, the peak at 348 cm^{-1} could

belong to the $CuIn_5S_8$ secondary phase grown from In–rich precursor solutions [20].

The broad band at 250 cm^{-1} correspond to the phonon vibration mode B2 observed in the chalcopyrite (CH) ordered phase of $CuInS_2$. The calculated and observed phonon vibration mode for Chalcopyrite and CuAu like structures in $CuInS_2$ are summarized in Table 5.

Table 5. Calculated and observed phonon frequencies in (cm^{-1}) for $CuInS_2$ Chalcopyrite(CH) and CuAu-like (CA)structures [20]

Structure	Symmetry of phonon mode	Calculated	Observed
$CuInS_2$ (CH)	B_2^2	241	234
	E^3	250	244
	A_1	285	294
Cu-Au (CA)	A_1^*	305	305

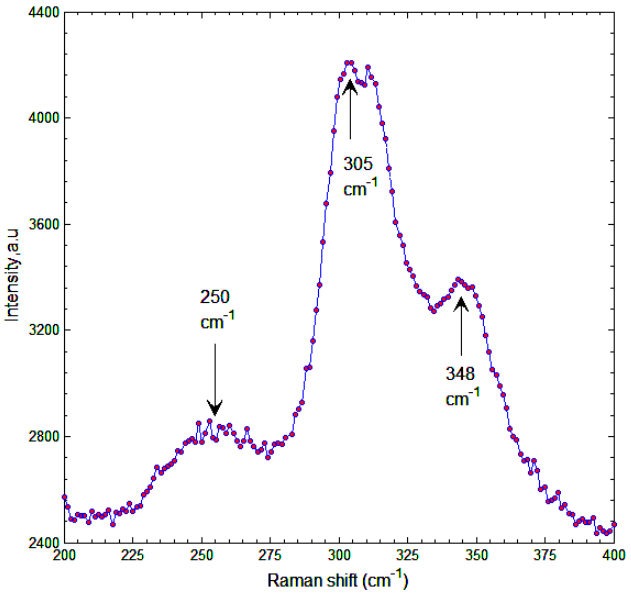

Fig. 9. Raman spectrum of as deposited $CuInS_2$,Cu/In=0.9

The Chalcopyrite (CH) and Copper Gold–like (Cu-Au) ordered structures shown in Fig. 10 are polytypes of $CuInS_2$ with the same composition. The two polymorphous structures can appear under thermodynamically different conditions [19]. An exceeding small formation energy difference ΔE_{form} = −1.95 meV/atom was found between chalcopyrite and CuAu like phases of $CuInS_2$. Therefore the two structures can coexist in the films [20]. The A_1 and A^*_1 Vibration modes were related to Cu-deficient $CuInS_2$ layers. Fig. 11 presents two vibration mode in $CuInS_2$.

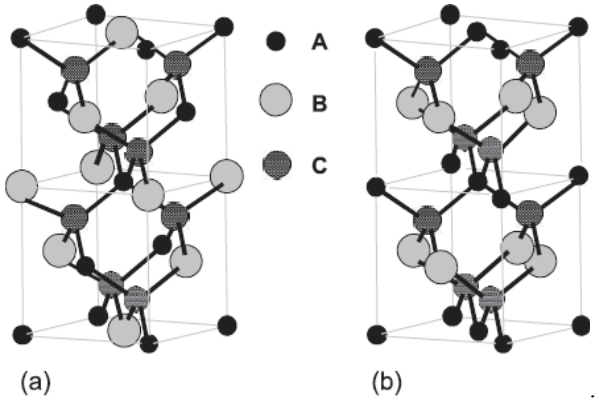

Fig. 10. Chalcopyrite(CH) (a) and Copper Gold(CuAu) (b) ordering in $A^IB^{III}C_2^{VI}$ compounds [17]

Similar results were obtained by Oja and coworkers [21]. Their Raman spectrum for as deposited Cu deficient $CuInS_2$, were fitted with lorentzians according to the results shown in Fig. 12. The most intensive band is splitted into two bands, A_1 band of chalcopyrite (CH) ordred compound at 290 cm^{-1} and A^*_1 band of CuAu (CA) ordering at 305 cm^{-1}.

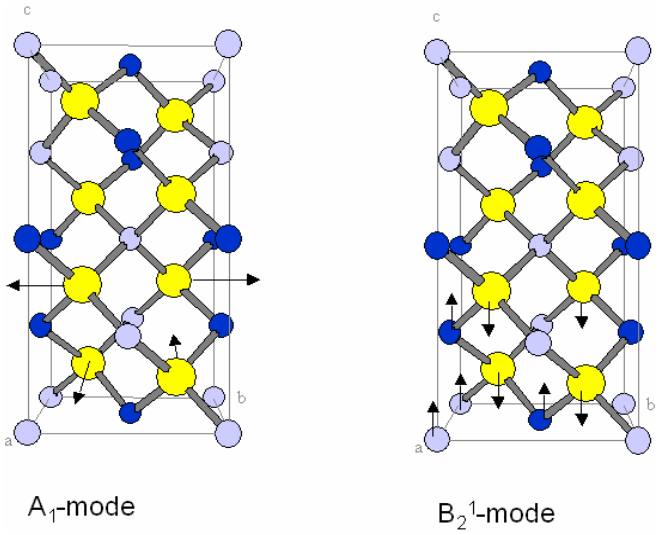

Fig. 11. A_1 and B_2 vibration modes in $CuInS_2$ [20]

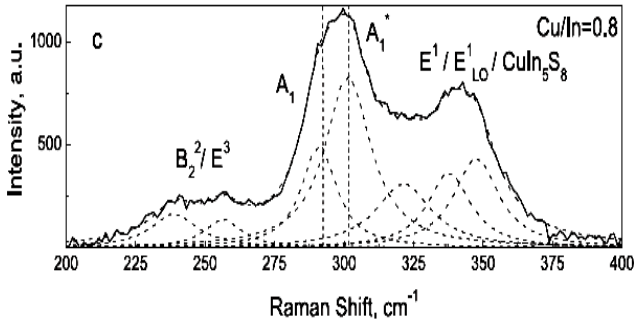

Fig. 12. Raman spectrum of $CuInS_2$, Cu/In=0.8[21]

4. Conclusion

Chalcopyrite polycrystalline thin films of copper indium disulfide were deposited by reactive Spray pyrolisis at 300°C. The molar cation ratio (Cu)/(In) was varied in the precursors solution. The elemental composition of the films was determined by EDAX. Hot probe method showed that samples with excess copper content in the film were p type whereas films grown under In rich condition were n type. The conductivity of films is controlled by the initial composition of the sprayed solution. Formation of intrinsic (native) defects in the grown CIS layers determine the doping of the films. Van der Pauw configuration were used to measure the resistivity of the samples. The increase of Copper to indium ratio in the initial solution results in increase in the conductivity. The concentration and mobility of the samples were determined by Hall effect method .The presence of high conductivity CuS and Cu_2S phases results in p type $CuInS_2$ thin films with degenerately high hole concentration. The Raman spectroscopy was used to analyse the vibration modes in the crystalline phase of the films. The intense peaks of 305 cm^{-1} reveals the CA ordered structure of $CuInS_2$ these findings correspond to copper deficient thins film. The Raman peak of 348 cm^{-1} corresponds to the $CuIn_5S_8$ phase. The Raman shift band at 260 cm^{-1} show the presence of Chalcopyrite structure in the deposited film. The broadening of Raman peaks is related to a high level of defects density in the obtained films.

Acknowledgements

This work is supported by all members of LMESM Laboratory.

References

[1] Peza Tapia, V. M. Sanchez, M. L. Abor, J. Cayente, Thin solid Films **490**, 142 (2005).
[2] H. Neumann, B. Schaman, D. Peters, A. Tempel, G. Kuhn, Crystal Res. Technol. **14**, 379 (1979).
[3] H. L. Hwang, C. L. Cheng, L. M. Liu, Y. C. Liu, C. Y. Sun, Thin Solid Films **67**, 83 (1980).
[4] A. N. Y. Samaan, S. Masim, A. E. Hill, D. G. Akmur, R. D. Tomlinson, Physica Status Solidi **96**, 317 (1986).
[5] M. Ortega-Lopez, Morales-Acevedo, Thin Solid Films **330**, 96 (1998).
[6] K. Subbaramaiah, V. S. Raja, Materials Letters **12**, 67 (1991).
[7] H. Metzner, M. Brüssler, K.-D. Husemann, H. J. Lewerenz, Phys. Rev. B **44**, 11614 (1991).
[8] S. B. Zhang, S. H. Wei, A. Zunger, H. Katayama Yoshida, Physical Review B **57**, 9642 (1998).
[9] H. Y. Ueng, H. L. Hwang, J. Phys. Chem. Solids **50**(12), 1297 (1989).
[10] G. Golan, A. Axelevitch, B. Gorenstein, V. Manevych, Microelectronics Journal **37**, 910 (2006).
[11] Kim, S. K. Jeong, W. J. Park, Synthetic Materials **71**, 1747 (1995).
[12] A. N. Tiwari, D. K. Pandya, K. L. Chopra, Thin Solid Films **130**, 217 (1985).
[13] D. K. Schroder, Semiconductor Materialand Device Characterization, Wiley, New York, 1990.
[14] E. A. Davis, N. F. Mott, Philos. Mag. **22**, 903 (1970).
[15] J. I. Pankove,Optical Processes in Semiconductors, Dover, New York, 1976.
[16] R. Scheer, R. Klenk, J. Klaer, I. Luck, Solar Energy **77**, 777 (2004).
[17] C. Guillen, J. Herrero, M. J. Gutierrez, F. Briones, Thin Solid Films **480-481**, 19 (2005).
[18] Yunbin He, $CuInS_2$ Thin films for Photovoltaic RF Reactive Sputter Deposition and Characterization, Dissertation, Giessen May 2003.
[19] Thomas Riedle, Raman Spectroscopy for the Analysis of thin $CuInS_2$ Films, Dissertation D83, Berlin 2002.
[20] J. A. Alvarez-Garcia, J. Marcos-Ruzafa, A. Pearez-Rodriguez, A. Romano-Rodriguez, J. R. Morante, R. Scheer, Thin Solid Films **361-362**, 208 (2000).
[21] I. Oja, M. Nanu, A. Katerski, M. Krunks, A. Mere, J. Raudojaa, A. Goossens, Thin Solid Films **480-481**, 82 (2005).

*Corresponding author: sahratoufik@gmail.com